Journal of the European Ceramic Society 22 (2002) 1767–1773

www.elsevier.com/locate/jeurceramsoc

^{57}Fe Mössbauer study of iron distribution in a kaolin raw material: influence of the temperature and the heating rate

O. Castelein[a], L. Aldon[b], J. Olivier-Fourcade[b], J.C. Jumas[b], J.P. Bonnet[a], P. Blanchart[a,*]

[a]*GEMH, Ecole Nationale Supérieure de Céramique Industrielle, 87065 Limoges Cedex, France*

[b]*Laboratoire des Agrégats Moléculaires et Matériaux Inorganiques (UMR 5072 CNRS), Université Montpellier II, Case Courrier 015, Place Eugène Bataillon, 34095 Montpellier Cedex 5, France*

Received 16 February 2001; received in revised form 26 October 2001; accepted 11 November 2001

Abstract

The thermal transformation of a kaolin raw material results from individual contributions of kaolinite and mica minerals, and from the complex nature of their mixture. In addition, it appears that the iron sites are subject to changes with the firing temperature and the heating rate, which influence the thermal transformations. Mössbauer spectroscopy provides information about iron site geometry and iron valence, and the resolution of this technique is high. For the kaolin studied, we determined the relative quantity of structural Fe^{III} and hematite as a function of temperature, up to 1100 °C and for two heating rates, 3 and 50 °C/min. Results indicate the loss of hematite above 900 °C and a subsequent increase of Fe^{III} in the structure of silico-aluminate phases. This trend is accentuated for a higher heating rate.

Keywords: Clays; Kaolin; Mössbauer spectroscopy; Thermal transformation

1. Introduction

Ceramic compositions for whitewares are mixtures of mainly silico-aluminate minerals and minor quantities of miscellaneous minerals. Iron is often a major impurity element, substituted for aluminium in silicate structures or associated in oxide and hydroxide compounds.

Kaolin raw materials are frequently used in such compositions. They are generally complex mixtures of kaolinite, a mica group mineral and quartz. The thermal behaviour is influenced by the minerals themselves, by the complexity of their mixture,[1] as well as by the iron impurity.[2] The latter can influence the structural reorganisation of the clay minerals and the sintering process.[3] For whitewares, the colour become undesirable when the iron amount is above about 1 wt.%; the fired material colour depends not only on the quantity, but also on the iron valency and structural environment.[4,5]

Rapid firing is often used during ceramic processes. Thermal cycles up to 10 °C/mn for porcelain or 50 °C/mn for tiles are usual. In the case of whitewares, this increases the complex character of sintering studies.[6] Some investigations have revealed the influence of heating rate on the thermal behaviour of a specific component in whiteware pastes, i.e. a kaolin raw material.[7–9] Particularly, the dehydroxylation and the structural reorganisation of clay minerals, the mullite formation process and the densification behaviour are significantly influenced when the firing rate changes. Furthermore, iron plays a significant role during these thermal transformations.

This study is devoted to the evolution of iron location and environment in a kaolin raw material during heating at constant rate. The investigations were carried out by Mössbauer spectroscopy, using a kaolin raw material fired at temperatures up to 1100 °C and using two heating rates, 3 and 50 °C/min.

2. Experimental

The kaolin raw material used, named Bio, is from Echassière in the centre of France. It is used for whiteware pastes. From X-ray diffraction and ICP analysis, the chemical and the mineralogical compositions are reported in Table 1.[1,10] We observe that impurities, as

* Corresponding author. Tel.: +33-5-5545-2222; fax: +33-5-5579-0998.

E-mail address: p.blanchart@ensci.fr (P. Blanchart).

0955-2219/02/$ - see front matter
PII: S0955-2219(01)00496-4

iron, are in reduced quantities and that the major phases are kaolinite mica and quartz minerals. The structural characteristics of the Bio kaolinite phase can be described by the Hincley index, the value of which is 0.97. It is very close to that of a typical well-crystallised kaolinite (Hincley index: 1). The structural characteristics of the mica phase are very similar to that of the $2M_1$ muscovite.[1,10] The quartz content (~4%) is low enough to influence very weakly the whole material properties.

The Bio samples were die pressed at 10 MPa (ϕ 13 mm, 2.5 mm thick), sintered at different temperatures and heating rates and then quenched to room temperature.

^{57} Fe Mössbauer spectra have been collected at room temperature in a standard transmission geometry using a standard constant acceleration EG & G spectrometer with a ^{57}Co(Rh) source. The velocity scale (±10 mm/s) is calibrated with reference to the magnetic sextet spectrum of a metallic iron foil absorber and all isomer shifts are given with respect to the centre of this spectrum. The absorbers were prepared from approximately 1.5 g of kaolin, grounded in a mortar (<40 μm) and placed in a lead sample holder (25 mm diameter, 2 mm thick). The signal to noise ratio was maximised during 4–5 days of data collection because of the low iron content (~1%).

All the Mössbauer spectra were fitted first to Lorentzian profiles by a least-squares method using the ISO fit programme.[11] For the Bio kaolin, we generally used one or more broad doublets (Fig. 1), characterised by an isomer shift (IS_D) and a quadrupole splitting (QS_D). An additional magnetically split sub-spectrum was also found, characterised also by a IS_D value and by a separation QS_D. It is as a six line pattern (sextet spectrum), which is related to the presence of magnetic particles [12] and the hyperfine field value (H) is calculated from QS_D value. On account of the line broadening an alternative fitting procedure was used in order to consider site distributions by calculating the quadrupole splitting p(QS) distribution or the hyperfine field distributions p(H) by means of the programme developed by Le Caer and Dubois.[13]

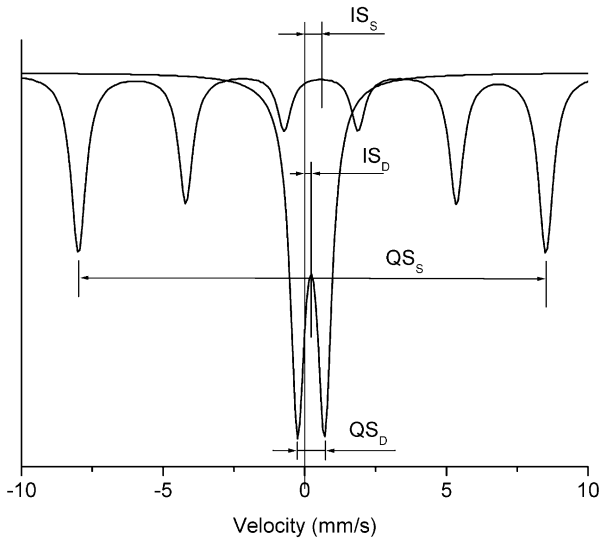

Fig. 1. Typical Mössbauer subspectra. A doublet D and a sextuplet S.

In kaolinite mineral, Al can be partially substituted by structural Fe. From Mössbauer investigations, the presence of octahedrally co-ordinated Fe^{III} is well established.[14] There is Fe^{II}, substituted trioctahedrally in the structure.[15–17] Furthermore, parameters of Mössbauer spectra, corresponding to Fe^{III} in kaolinite tetrahedral sites have been published.[18] Typical data for Mössbauer spectra parameters of kaolinite are indicated in Table 2.

Structural Fe can also be present in muscovite mica, particularly in the typical $2M_1$ polytype which is often associated with kaolinite in kaolin raw materials. Fe^{III} and Fe^{II} populations are distributed in cis and trans octahedral sites[19,20] which can be distinguished in Mössbauer spectra. The individual parameters of Fe ions in both sites of muscovite are indicated in Table 3. However, an attempt to separate the two populations is

Table 1
Chemical and mineralogical composition of Bio kaolin

Wt.%	Bio	Bio minerals	Wt.%
SiO_2	47.10	Kaolinite	79±2
Al_2O_3	36.70	Muscovite	17±2
Fe_2O_3	1.16	Quartz	4±1
TiO_2	0.07		
CaO	0.11		
MgO	0.21		
Na_2O	0.11		
K_2O	2.17		
Li_2O	0.11		
P_2O_5	–		
Loss on ignition	12.26		

Table 2
Data of Mössbauer parameters for structural iron in kaolinite mineral

	IS (mm/s)	QS (mm/s)
Fe^{III} octahedral	0.37	0.58
Fe^{II} octahedral	1.00	2.39
Fe^{III} tetrahedral	0.2	1

Table 3
Data of Mössbauer parameters for structural iron in muscovite mineral

	IS (mm/s)	QS (mm/s)
Fe^{II} octahedral in *trans* site	1.30	3.0
Fe^{II} octahedral in *cis* site	1.03	2.6
Fe^{III} octahedral in *trans* site	0.40	0.97
Fe^{III} octahedral in *cis* site	0.01	0.67

only possible when well resolved individual contributions are available [19], i.e. when site or vacancy disorder are sufficiently reduced to avoid signal overlapping.

Iron oxides or hydroxides are often detected in kaolin raw materials.[21] The most widely occurring Fe oxides are hematite, mostly as very fine particles[22] or goethite, adsorbed on kaolinite surfaces.[15,23] Among a large number of possible iron species, lepidocrocite phase[24] or hematite partially substituted by Al[25] have also been found.

In the Bio material, for complementary experiments, the major parts of the iron oxides and hydroxides were removed, using a sequence of three chemical extractions with dithionite–citrate–carbonate solution[26](DCB). This method was successfully used elsewhere with kaolin raw materials[27] and kaolinitic clays[2], to provide specific information on structural iron.

3. Results

Fig. 2. shows the Mössbauer spectrum of the raw Bio kaolin at room temperature. It is composed of two distinctive doublets having very different isomer shifts and quadrupole splittings. One can be associated with Fe^{III} (IS = 0.23 mm/s and QS = 0.95 mm/s). Here the low value of IS is characteristic of octahedral iron in kaolinite and muscovite, but a small contribution from tetrahedral iron is possible. The other doublet (IS = 1.16 mm/s and QS = 2.85 mm/s), is related to the dominant part of iron. It corresponds to octahedral Fe^{II}, which is assumed to be structural, or to the surface iron of muscovite. An additional sextet is also found, having a magnetic hyperfine field of 477 kOe, an isomer shift (IS) of 0.39 mm/s and a quadrupole splitting (QS) of −0.167 mm/s. These data are close to data for natural hematite: 0.37 mm/s for IS ;−0.20 mm/s for QS; 518 kOe for the magnetic hyperfine field.[28] For our samples, the magnetic hyperfine field is too large to be due to goethite.

After DCB treatment (Fig. 3), only a very broad doublet remains, the IS value of which (0.38 mm/s) is characteristic of Fe^{III} (Table 2). The sextet absence indicates the removal of iron oxides and iron hydroxides, but the Fe^{II} species was also removed by the chemical treatment. This may therefore have been an iron coating on the muscovite layers.

All these iron contributions are calculated from relative surfaces of respective subspectra (C), which are related to atom quantities. They are indicated in Table 4 and plotted in Fig. 4.

After heating at 600 °C, using a 3 °C/min heating rate, the contribution of the magnetically split sextets from the magnetic iron is increased. Simultaneously, the octahedral Fe^{II} is transformed into Fe^{III} octahedral species, the characteristics of which are different from those observed at room temperature. Using a 50 °C/min heating rate, the hematite quantity increases weakly. Simultaneously, the octahedral Fe^{II} is reduced to form octahedral Fe^{III}.

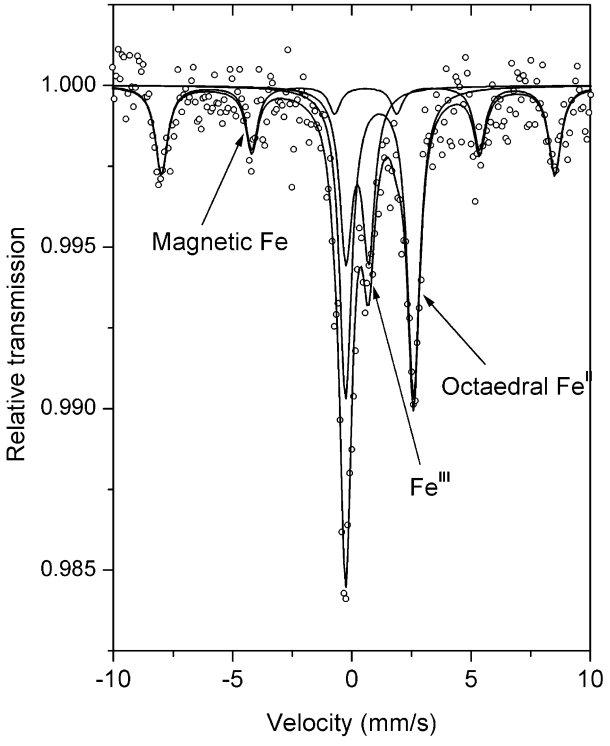

Fig. 2. Mössbauer spectrum of the raw Bio kaolin. Experimental data and simulation.

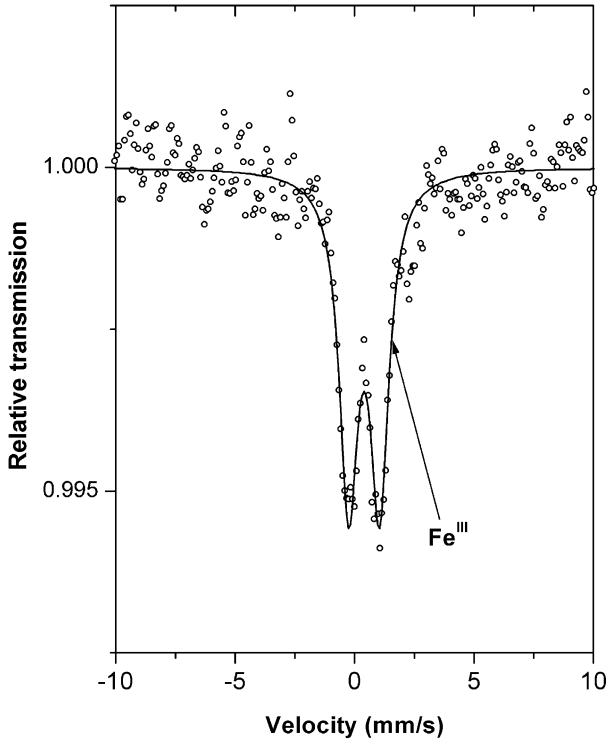

Fig. 3. Mössbauer spectrum of the treated Bio kaolin, using DCB.

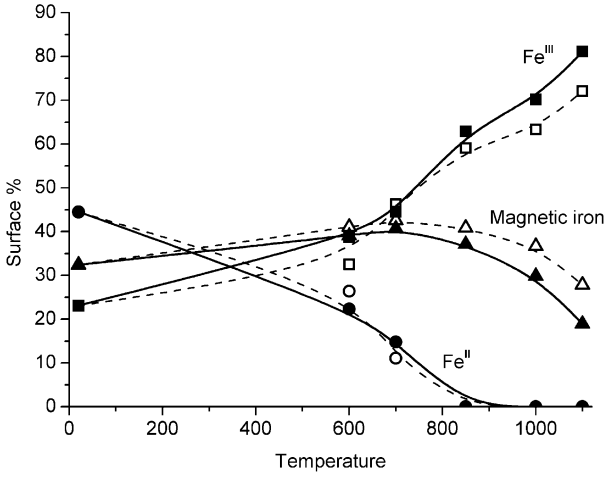

Fig. 4. Individual contributions of species to the total surface, against temperature. Dashed line and open symbols: 3 °C/min; solid line and closed symbols: 50 °C/min. ■, Fe^{III}; ▲, Fe_2O_3; (●): Fe^{II}.

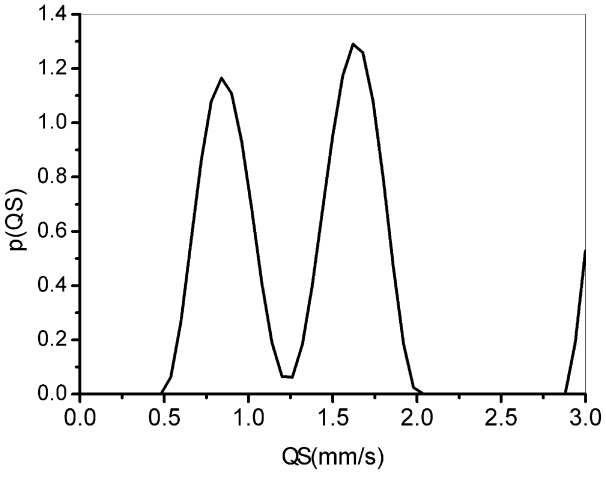

Fig. 5. QS values of Fe^{III} sites for the raw Bio kaolin.

Over 600–850 °C temperature range, Fe^{II} is reduced drastically and Fe^{III} increases continuously, particularly with the 50 °C/min heating rate. Simultaneously, the magnetic iron attains its maximum value at about 850 °C.

At the highest temperatures, 1000–1100 °C, the octahedral Fe^{III} is the most important iron species. The very broad doublets are characterised by a reduction of IS, which indicates the presence of complex structures with iron. The magnetic iron quantity is reduced with characteristics close to those of pure iron.

In Table 4, we indicated all experimental values of relative surfaces (C) for each subspectra. Corresponding IS and QS for doublets and $<H>$ for sextuplets are also tabulated.

4. Discussion

The broad lines of the Mössbauer spectra can be alternatively fitted by constraining the line width of doublets to be equal to that of iron (0.34 mm/s). This improves the resolution of the various site populations of magnetic iron.

For the raw kaolin spectrum, the large Fe^{III} doublet of Fig. 2 is simulated by two narrow doublets corresponding to two different structural Fe^{III} sites. QS values are 0.84 1.62 mm/s (Fig. 5), while IS remains close to 0.38 mm/s. From a comparison with data from Tables 2 and 3, it can be admitted that Fe^{III} is present inside two different site types, either in the octahedral sites of kaolinite and cis sites of muscovite (for QS = 0.84 mm/s) or in trans sites of muscovite (for QS = 1.62×mm/s).

The distribution of magnetic components can be analysed against the magnetic hyperfine field. Results are presented for the raw Bio kaolin in Fig. 6, as a function of temperature and heating rate. Three significant values of the magnetic hyperfine field are pointed out, at 388–490 and 516 kOe. The 388.4 and 516.1 kOe field sites can be ascribed to αFeOOH[15,23] and hematite αFe_2O_3[22] respectively. For the intermediate value of 489.8 kOe, a hematite substituted structure $Fe_{2-x}Al_xO_3$ can be proposed.[25]

In Fig. 6, the distribution of the magnetic hyperfine field is obviously modified when the temperature and the heating rate change. The 388 kOe peak, corresponding to goethite, disappears below 700 °C and the relative surface (C) for the 516 kOe peak, for hematite, is largely modified. Individual contributions of sextets to the total surface area are indicated in Table 4 and plotted in Fig. 7.

Below 700 °C, the increase of the heating rate changes the site type of Fe from that of goethite. At 3 °C/min, it transformed mainly into the substituted structure $Fe_{2-x}Al_xO_3$ (Fig. 7). At 50 °C/min, a similar species is also formed, together with Fe_2O_3 (Fig. 7).

From 700 to 850 °C, for 3 °C/min, the $Fe_{2-x}Al_xO_3$ species is progressively changed into Fe_2O_3, which attains the maximum value of 35% (Fig. 7). In this temperature range, the magnetic hyperfine field spectrum is similar, which means a limited structural and chemical change of the iron oxides. For 50 °C/min, the Fe_2O_3 quantity decreases progressively, but the other species remain at a quasi-constant content (Fig. 7). The magnetic hyperfine field corresponding to the $Fe_{2-x}Al_xO_3$ decreases with temperature, indicating a stoechiometry variation, probably an increase of aluminium content. From these findings, it can be proposed that a correlation exist between the iron species quantities, between 600 and 700 °C, and the end of the dehydroxylation process of the Bio kaolinite, at about 650 °C. This correlation is evidenced in Fig. 7.

Above 850 °C, the hematite quantity decreases in all cases (Fig. 7), to favour structural Fe^{III} (Fig. 4). At 3 °C/min, the Fe from Fe_2O_3 becomes structural Fe^{III}. But at 50 °C/min, the increase of structural Fe^{III} is due to both

Table 4
Mössbauer parameters for doublets (IS and QS) and for sextuplets (<H>) in Bio kaolin, as a function of the temperature and the temperature rate. The (<H>) distribution and the corresponding distribution of magnetic species are also indicated as: [1] αFeOOH; [2] $Fe_{2-x}Al_xO_3$; [3] hematite

Sample	Thermal treatment	IS (mm/s)	QS (mm/s)	<H> (kOe)	C (%)	Specie
Bio raw material	Room temperature	0.23	0.95	–	23.1	Fe^{III}
		1.16	2.85	–	44.5	Fe^{II}
		0.39	−0.167	477.6	32.4	Magnetic iron
				388.4	8.7	[1]
				489.8	1.5	[2]
				516.1	22.2	[3]
Bio treated with CDB	Room temperature	0.38	0.84	–	∼50	Fe^{III}
Bio raw material	600 °C	0.35	1.13	–	32.5	Fe^{III}
	3 °C/min	1.21	2.91	–	26.4	Fe^{II}
		0.412	−0.119	478.3	41.1	Magnetic iron
				439.7	6.2	[1]
				489.2	11	[2]
				515.5	23.9	[3]
	600 °C	0.38	1.17	–	38.7	Fe^{III}
	50 °C/min	1.21	2.88	–	22.3	Fe^{II}
		0.360	−0.091	489.4	39.0	Magnetic iron
				468.7	5.7	[1]
				500.3	5.8	[2]
				513.5	27.6	[3]
	700 °C	0.32	1.26	–	46.3	Fe^{III}
	3 °C/min	1.08	2.58	–	11.1	Fe^{II}
		0.359	−0.114	485.0	42.6	Magnetic iron
				465.4	3.6	[1]
				492.5	5.8	[2]
				515.5	33.1	[3]
	700 °C	0.32	1.26	–	44.5	Fe^{III}
	50 °C/min	1.08	2.58	–	14.8	Fe^{II}
		0.359	−0.114	484.7	40.7	Magnetic iron
				433.2	7.4	[1]
				493.7	6.1	[2]
				514.8	27.3	[3]
	850 °C	0.36	1.49	–	59.1	Fe^{III}
	3 °C/min	0.364	−0.121	493.6	40.9	Magnetic iron
				464.7	4.4	[1]
				488.2	1.7	[2]
				514.2	34.8	[3]
	850 °C	0.37	1.13	–	62.9	Fe^{III}
	50 °C/min	0.371	−0.099	483.4	37.1	Magnetic iron
				435.8	5.6	[1]
				483.9	6.9	[2]
				514.2	24.7	[3]
	1000 °C	0.30	1.05	–	63.3	Fe^{III}
	3 °C/min	0.375	−0.130	487.4	36.7	Magnetic iron
				377.9	2.8	[1]
				465.4	2.8	[2]
				514.8	31.1	[3]
	1000 °C	0.30	0.93	–	70.2	Fe^{III}
	50 °C/min	0.362	−0.098	486.8	29.8	Magnetic iron
				443.7	1.7	[1]
				481.8	4.7	[2]
				511.5	23.5	[3]
	1100 °C	0.30	0.97	–	72.1	Fe^{III}
	3 °C/min	0.369	−0.144	492.7	27.9	Magnetic iron
				428.5	1.5	[1]
				–	–	[2]
				516.1	26.4	[3]
	1100 °C	0.24	1.04	–	81.1	Fe^{III}
	50 °C/min	0.360	−0.121	498.5	18.9	Magnetic iron
				–	–	[1]
				466.0	2.0	[2]
				514.0	16.9	[3]

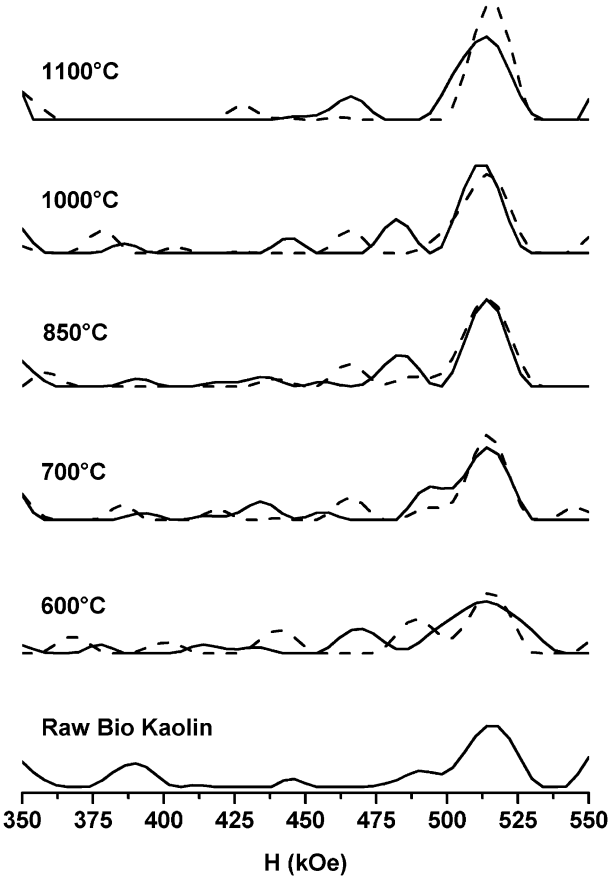

Fig. 6. Distribution of <H> relative to sextuples, for the raw Bio kaolin, as a function of temperature and temperature rate. Dashed line: 3 °C/min; solid line: 50 °C/min.

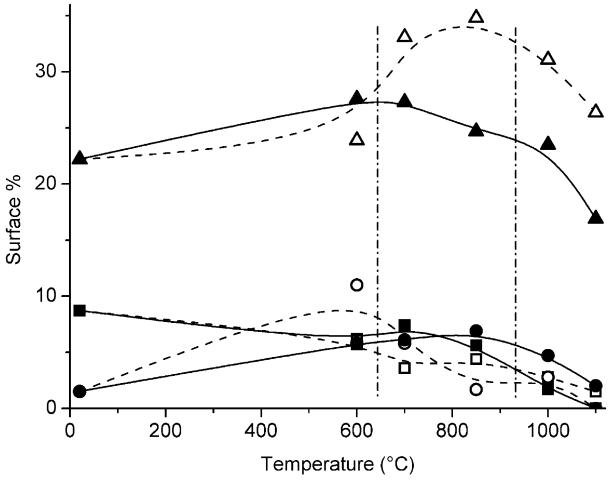

Fig. 7. Relative surface for magnetic components, against temperature and temperature rate. Dashed line and open symbols: 3 °C/min; solid line and closed symbols: 50 °C/min. ■, αFeOOH; ●, $Fe_{2-x}Al_xO_3$; ▲, hematite.

Fe_2O_3 and $Fe_{2-x}Al_xO_3$. Here, an interesting correlation is found with the beginning of the structural reorganisation stage of the kaolinite mineral, the temperature of which is indicated in Fig. 7.

Fig. 8. TEM observation of kaolinite transformed phase, fired at 1050 °C, indicating the presence of iron rich clusters. Bar = 100 nm.

In the 850–1100 °C temperature range, it was found that a part of the Fe^{III} is in the Bio kaolinite transformed phase. This observation was correlated with the TEM observation of a Bio kaolin sample fired at 1100 °C. It shows a kaolinite particle, which includes iron rich clusters of about 20–50 nm (Fig. 8). The nature of these phases was clearly identified by microanalysis as iron oxide. In that case, the iron presence suggests a role in the structural reorganisation of the metakaolin phase. Particularly, the iron site type and quantity should be related to the mullite nucleation mechanisms, above 900 °C. In fact, it was shown elsewhere that the mullite crystallite quantity increases in the metakaolin transformed phase at a high firing rate.[7]

Muscovite mineral contains the most part of the initial structural iron. This element is transformed in situ and it is rather unlikely that iron from muscovite diffuses at long distance even at low temperature rates. This assumption is supported by the large initial particle size of muscovite in Bio kaolin and by the reduced interaction between kaolinite and mica minerals at high temperature rates.[10] Above 850 °C, in a similar way as for kaolinite, the end of the dehydroxylation stage of muscovite mineral[29] is correlated with the significant transformation of iron species.

5. Conclusion

Although the complex nature of a raw kaolin, Mössbauer spectroscopy was successfully applied to the

identification of iron distribution during the thermal transformations. The site types of iron are modified when the temperature and the heating rate vary. The most part of iron in the raw kaolin is distributed in both kaolinite and muscovite minerals, but also in hematite and goethite phases. When the temperature increases up to 700 °C, a progressive transformation of Fe^{II} to octahedral Fe^{III} is observed. Simultaneously, the hematite quantity, which is initially low, increases, to attain almost 40% of the total iron content. Above 700 °C, the hematite quantity decreases and the structural Fe^{III} in a silico aluminate phase becomes predominant. Temperatures of the most significant transformations of iron site changes are correlated with the thermal transformations of the clay minerals. An increase of the heating rate favours a reduction of hematite content and an increase in structural Fe^{III}.

References

1. Castelein, O., Bonnet, J. P. and Blanchart, P., Comparison between high temperature behaviours of a kaolin raw material and reference mineral. *Annales de Chimie Science des Matériaux*, 2000, **25**(Suppl. 1), 241–245.
2. Sei, J., *Etude de Matériaux de Dimensionalité réduite. Relation Structure-Propriétés dans des Kaolinites Naturelles de Côte d'Ivoire*, PHD thesis, Montpellier University, 1998.
3. Johnson, S. M. and Pask, J. A., Rôle of impurities on formation of mullite from kaolinite and Al_2O_3–SiO_2 mixtures. *Ceram. Bull.*, 1982, **61**(8), 838–842.
4. Carceller, J. V., Soler, A., Nebot, A., Garcia-Belmonte, G., Fabregat, F. and Carda, J. B., Influence of variations in kiln atmosphere on fired tile quality in ceramic processes in general, and in porous single fired in particular. *Int. Ceram. J.*, 1998, **2**, 22–29.
5. Murad, E. and Wagner, U., The thermal behaviour of an Fe-rich illite. *Clay Minerals*, 1996, **31**, 45–52.
6. Slosarczyk, A. and Hennicke, H. W., The influence of fast firing on triaxial porcelain containing silica raw materials from different origins. *Interceram.*, 1986, **1**, 15–17.
7. Dion, P., Alcover, J. F., Bergaya, F., Ortega, A., Llewellyn, P. L. and Rouquerol, F., Kinetic study by controlled-transformation rate thermal analysis of the dehydroxylation of kaolinite. *Clay Minerals*, 1998, **33**, 269–276.
8. Carty, W. M. and Senapati, U., Porcelain-raw materials, processing, phase evolution, and mechanical behaviour. *J. Am. Ceram. Soc.*, 1998, **81**(1), 3–20.
9. Castelein, O., Soulestin, B., Bonnet, J. P. and Blanchart, P., The influence of heating rate on the thermal behaviour and mullite formation from a kaolin raw material. *Ceramics International*, 2001, **27**(5), 517–522.
10. Castelein, O. *Influence de la Vitesse du Traitement Thermique sur le Comportement d'un Kaolin: Application au Frittage Rapide*, PHD thesis, Limoges University, 2000.
11. Künding, W., A least-square fit program. *Nucl. Instr. Meth.*, 1969, **75**, 336–340.
12. Murad, E. and Wagner, U., Clay and clay minerals: the firing process. *Hyperfine Interactions*, 1998, **117**, 337–356.
13. Le Caer, G. and Dubois, J. M., Evaluation of hyperfine parameter distributions from overlapped Mössbauer spectra of amorphous alloys. *J. Phys. E : Sci. Instrum.*, 1979, **12**, 1083–1090.
14. Malden, P. J. and Meads, R. E., Substitution by iron in kaolinite. *Nature*, 1967, **215**, 844–846.
15. Jefferson, D. A., Tricker, M. J. and Winterbottom, A. P., Electron microscopy and Mössbauer spectroscopic studies of iron-stained kaolinite minerals. *Clays and Clay Minerals*, 1975, **23**, 355–360.
16. Murad, E. and Wagner, U., Mössbauer spectra of kaolinite, halloysite and the firing products of kaolinite. *N. Jahrb. Miner.*, 1991, **162**, 281–309.
17. Cuttler, A. H., The behaviour of a synthetic 57Fe doped kaolin: Mössbauer and electron paramagnetic resonance studies. *Clay Miner.*, 1980, **15**, 429–444.
18. Petit, S. and Decarreau, A., Hydrothermal synthesis and crystal chemistry of iron-rich kaolinites. *Clay Miner.*, 1990, **25**, 181–196.
19. Shabani, A. A. T., Rancourt, D. G. and Lalonde, A. E., Determination of cis and trans Fe^{2+} populations in $2M_1$ muscovite by Mössbauer spectroscopy. *Hyperfine Interactions*, 1998, **117**, 117–129.
20. Schmidt, W. and Pietzsch, C., Iron distribution and geochemistry of pegmatitic dioctaedral $2M_1$ micas. *Chem. Erde*, 1990, **50**, 27–38.
21. Hogg, C. S., Malden, P. J. and Meads, R. E., Identification of iron containing impurities in naturral kaolinites using the Mössbauer spectroscopy effect. *Min. Mag.*, 1975, **40**, 89–96.
22. Janot, C., Gibert, H. and Tobias, C., Caracterisation de kaolinites ferrifères par spectroscopie Mösbauer. *Bull. Soc. Fr. Mineral. Cristallogr.*, 1973, **96**, 281–291.
23. Fysh, S. A. and Clark, P. E., Aluminous goethite, a Mössbauer study. *Phys. Chem. Minerals*, 1982, **8**, 180–187.
24. Angel, B. R. and Vincent, W. E. J., Electron spin resonance studies of iron oxides associated with the surface of kaolinite. *Clay Miner.*, 1978, **26**, 263–272.
25. Fysh, S. A. and Clark, P. E., Aluminous hematite, a Mössbauer study. *Phys. Chem. Minerals*, 1982, **8**, 257–267.
26. Aguilera, N. H. and Jackson, M. L., Iron oxide removal from soils and clays. *Soil Sci. Proc.*, 359–364.
27. St Pierre, T., Singh, B., Webb, J. and Gelkes, B., Mössbauer spectra of soil kaolins from south-western Australia. *Clays and Clay Miner.*, 1992, **40**(3), 341–346.
28. Murad, E., Clay and clay minerals: what can Mössbauer spectroscopy do to help understand them. *Hyperfine Interactions*, 1998, **117**, 39–70.
29. Mackenzie, R. C., Differential Thermal Analysis. Academic Press, 1970.